Nano World Journal

https://doi.org/10.17756/nwj.2023-s4-089

Research Article

Open Access

Structural and Electrical Properties of (1-x)$BiFeO_3$ – x$Na_{0.5}Bi_{0.5}TiO_3$ Ceramics

M. Sudhadhar[1], G. Bhavani[1], Ch. Komala Lakshmi[1], B. Sattibabu[1], T. Karthik[2], Saket Asthana[3], Ch. V. Koti Reddy[1] and T. Durga Rao[1*]

[1]Department of Physics, School of Science, GITAM (Deemed to be University), Visakhapatnam, Andhra Pradesh, India
[2]Centre for Materials for Electronics Technology (C-MET), Ministry of Electronics and Information Technology (MeitY), Thrissur, Kerala, India
[3]Advanced Functional Materials Laboratory, Department of Physics, Indian Institute of Technology, Hyderabad, Telangana, India

[*]Correspondence to:
T. Durga Rao
Department of Physics,
School of Science,
GITAM (Deemed to be University),
Visakhapatnam, Andhra Pradesh, India.
E-mail: dtadiset@gitam.edu

Received: September 19, 2023
Accepted: December 05, 2023
Published: December 08, 2023

Citation: Sudhadhar M, Bhavani G, Lakshmi ChK, Sattibabu B, Karthik T, et al. 2023. Structural and Electrical Properties of (1-x) $BiFeO_3$ –x$Na_{0.5}Bi_{0.5}TiO_3$ Ceramics. *NanoWorld J* 9(S4): S524-S527.

Copyright: © 2023 Sudhadhar et al. This is an Open Access article distributed under the terms of the Creative Commons Attribution 4.0 International License (CCBY) (http://creativecommons.org/licenses/by/4.0/) which permits commercial use, including reproduction, adaptation, and distribution of the article provided the original author and source are credited.

Published by United Scientific Group

Abstract

The ceramic compounds (1-x)$BiFeO_3$–x$Na_{0.5}Bi_{0.5}TiO_3$, x = 0.05, 0.10 and 0.15 were prepared. Rietveld refinement using full-prof software indicates that the compounds exhibited in *R3c* rhombohedral structure. By using the complex impedance studies, the grain and grain boundary resistances were found to decrease with the increase of temperature, whereas it increases with the increase of x. Non-Debye type relaxations were observed from impedance as well as from modulus studies. The *ac* conductivity studies were conducted to investigate the insulating character of compounds.

Keywords

Ceramics, X-ray diffraction, Impedance

Introduction

Ferroelectricity and (anti)ferromagnetism co-exist in single phase material is observed in multiferroics. This is found to be quite interesting for applications in technology such as spintronics, microelectronics and memory devices [1, 2]. However, the abundance of these materials is very scarce because of the so called d^0 vs d^n problem [3]. The *d*-orbital of transition metals or *f*-orbital of rare earth elements should be partially filled to have ferromagnetic properties. The ferroelectricity will originate from various mechanisms such as off-centering of transition metal ions with empty *d*-orbital, lone pair mechanism, charge ordering, etc. Bismuth ferrite ($BiFeO_3$) (BFO) is a one of the fascinating materials rich in physics in the known multiferroics. BFO is a room temperature multiferroic with high T_c = 1103 K and high T_N = 643 K [4]. The crystal structure of BFO is reported with *R3c* space group having rhombohedral structure. However, the main concerns of BFO are (i) formation of single phase BFO, (ii) high leakage currents, (iii) weak ferromagnetism. Several strategies have been incorporated in order to deal with these issues such as (i) adapting different synthesis techniques, (ii) doping of elements at A/B – sites, (iii) formation of composites [5-7]. On the other hand, sodium bismuth titanate ($Na_{0.5}Bi_{0.5}TiO_3$) (NBT) is a lead-free ferroelectric material with large remanent polarization and high T_c [8]. It is exhibited in *R3c* rhombohedral structure. Further, it is also reported that making solid solution of BFO with NBT, an interesting magnetic, ferroelectric, and dielectric properties are observed [9, 10]. In this work, we synthesized the solid solution of BFO with NBT and studied their structural and electrical properties through impedance measurements.

The structural and electrical properties of(1-x)$BiFeO_3$–x$Na_{0.5}Bi_{0.5}TiO_3$ ceramics using nanotechnology involves a sophisticated exploration at the nanoscale level, offering unique insights into the material's characteristics. Nanostructured ceramics can be synthesized using various techniques, such as sol-gel processes or high-energy ball milling, to achieve enhanced properties. The composition (1-x)$BiFeO_3$–x$Na_{0.5}Bi_{0.5}TiO_3$ represents a solid solution of BFO and NBT. The nanotechnology aspect comes into play during the fabrication process, aiming to control particle size and distribution, thereby influencing the resulting material's properties. The nanosized grains and interfaces can significantly impact structural features, such as phase composition, crystallinity, and grain boundaries. The use of nanotechnology in this context allows for tailoring the material's characteristics to optimize its performance for potential applications in electronic devices, sensors, or energy harvesting systems. Advanced characterization techniques, including X-ray diffraction (XRD), electron microscopy, and impedance spectroscopy, can be employed to thoroughly analyze the structural and electrical aspects of these nanoengineered ceramics.

Experimentation

Polycrystalline (1-x)BFO–xNBT, x = 0.05 (NBT5), 0.10 (NBT10), and 0.15 (NBT15) samples were synthesized by using Bi_2O_3, Fe_2O_3, $NaCO_3$ and TiO_2 oxides as starting materials and mixed according to their stoichiometric ratios. The powders were calcined at 800 °C for 5 h. The heated powders were made as pellets and carried out sintering at 850 °C for 5 h. Panalytical X'pert Pro was used to study the XRD measurements. Impedance measurements were carried out on the compounds using impedance analyzer (Wayne Kerr 6500B) with temperature and frequency variations.

Results and Discussion

Structural studies

The XRD patterns of NBT5, NBT10 and NBT15 compounds are shown in figure 1. The crystal structure of all compounds is observed to be rhombohedral as is evidenced from the XRD patterns [4]. $Bi_2Fe_4O_9$ and $Bi_{25}FeO_{40}$ are the secondary phases which appear to be suppressed with the increase of x. Rietveld refinement also confirmed the crystal structures of the compounds. The values of lattice parameters obtained from refinement are, a = 5.5794 Å and c = 13.8709 Å for NBT5, a = 5.5734 Å and c = 13.8393 Å for NBT10 and a = 5.5714 Å and c = 13.8239 Å for NBT15. Increase in lattice parameters are observed which could be due to the higher ionic sizes of Na^+ (1.39 Å) ions than that of Bi^{3+} (1.38 Å) ions.

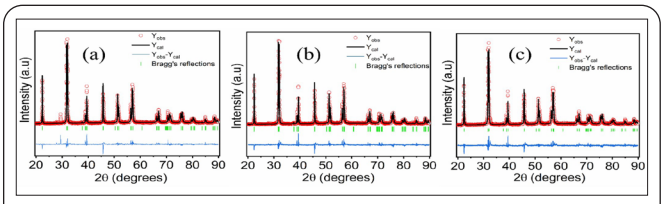

Figure 1: XRD patterns of **(a)** NBT5, **(b)** NBT10, and **(c)** NBT15 compounds. The asterisks # and * respectively represent $Bi_{25}FeO_{40}$ and $Bi_2Fe_4O_9$, respectively.

Impedance studies

Frequency variation of Z′ (real part of impedance) of NBT5, NBT10 and NBT15 is measured (not shown here). In the low frequency regions, the dielectric relaxation behavior is reflected from the dispersion of Z′. The increase in Z′ with the increase of NBT content indicates an increase in bulk resistance of the compound. The frequency variation of Z″ (imaginary part of impedance) of NBT5, NBT10 and NBT15 compounds is shown in figure 2. Above 165 °C, the frequency variation of Z″ plot exhibit (i) a peak in Z″ (i.e., Z''_{max}) confirming presence of electrical relaxations, (ii) an asymmetrical broadening due to the distribution of relaxation times, and (iii) Z''_{max} shifts towards high frequency side with temperature [11]. It is observed that as the NBT content increases in BFO, Z″ increases and Z''_{max} shifts towards lower frequency side indicating the phenomenon of maximum capacitive effects.

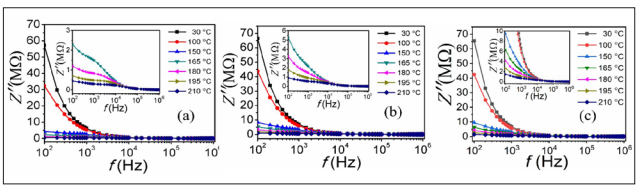

Figure 2: The frequency variation of the imaginary part of impedance (Z″) of **(a)** NBT5, **(b)** NBT10, and **(c)** NBT15 compounds.

In order to estimate the gran resistance (R_g) and grain boundary resistance (R_{gb}), the variation of Z″ with Z′ (Nyquist plots) is plotted and shown in figure 3 for all compounds. In the Nyquist plots the semi-circular arc intercepts on Z′-axis directly measures of bulk resistance of the compounds. The semi-circular arc intercepts decrease with the increase in temperature. It means that as temperature increases there is a decrease in the bulk resistance of the compounds and exhibits negative temperature coefficient of resistance (NTCR) character. The depressed semi-circular arcs appear which indicates a non-Debye type relaxations in the compounds.

Above 165 °C, Z″ vs Z′ data is fitted with two R-C parallel circuit model as per brick-layer model to extract R_{gb} and R_g. The values of R_g and R_{gb} were extracted from the fitting of Nyquist's plots are given in table 1. Both R_{gb} and R_g decrease with the increase of temperature and show the NTCR character is consistent with the Z′ data. A higher R_{gb} than R_g indicates that grain boundaries offer higher contribution to the bulk resistance of the compound than the grains. Both R_{gb} and R_g increase with the increase of NBT content at any temperature.

Electric modulus studies

The variation of the imaginary part of electric modulus (M″) with frequency is shown in figure 4. M″ is evaluated us-

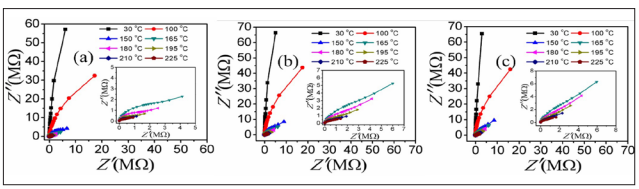

Figure 3: Z″ vs Z′ for **(a)** NBT5, **(b)** NBT10, and **(c)** NBT15 compounds at different temperatures.

Table 1: R_g and R_{gb} values extracted from Nyquist's plots at different temperatures.

Compound	Temperature (°C)	R_{gb} (MΩ)	R_g (MΩ)
NBT5	165	11.9	4.51
	180	7.19	2.43
	195	3.98	1.32
	210	2.39	0.79
	225	1.54	0.457
	240	1.176	0.255
NBT10	165	32.6	6.15
	180	26.2	3.14
	195	15.7	1.86
	210	7.04	1.19
	225	3.18	0.72
	240	2.02	0.38
NBT15	165	43	5.83
	180	36.7	3.27
	195	22.2	1.98
	210	12.7	1.18
	225	5.41	0.7
	240	2.66	0.4

ing the equation 1.

$$M'' = \omega C_O Z' \quad (1)$$

Where ω is angular frequency, C_o is the empty capacitance. M″ curves show (i) a peak at a frequency (M''_{max}), (ii) peak broadening, and (iii) shifting of M''_{max} towards higher frequency side with the temperature. The frequency ω and M''_{max} follows equation 2.

$$\omega_{max} = \omega_O e^{-Ea/kT} \quad (2)$$

Where ω_o and E_a are constant and activation energy respectively. The values of E_a are calculated by fitting the above equation. The values of E_a of NBT5, NBT10 and NBT15 are 0.69, 0.67 and 0.53 eV, respectively. The values of activation energy that are observed show that oxygen vacancies will be the prime charge carriers for conduction in all the compounds [12].

ac conductivity studies

For understanding the insulating character and nature of the transport process, the studies of *ac* conductivity are very useful. The *ac* conductivity can be calculated from equation 3.

$$\sigma(\omega) = \varepsilon_o \varepsilon_r \omega \tan\delta \quad (3)$$

Where is ε_r dielectric constant and is tan δ loss tangent.

The dependance of *ac* conductivity on frequency at different temperatures is shown in figure 4. In all the compounds the increase of *ac* conductivity with the increase of temperature indicates that the compounds exhibit NTCR character. These observations are in corroboration with the impedance findings. At any given temperature, the *ac* conductivity decreases with the increase in NBT content. The decrease in conductivity means the improved insulating character with the NBT content. The decrease in conductivity may arise due to reduction of oxygen vacancies and/or improved grain boundaries. The decrease in oxygen vacancies can be anticipated because of the empty *d*-orbital of Ti^{4+} ions. The movement of charge carriers is hindered due to the obstacles of Ti^{4+} ions and the grain boundaries and hence the decrease in conductivity.

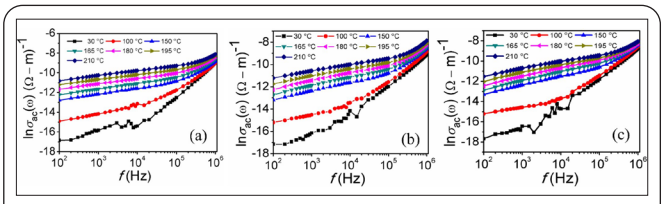

Figure 4: The frequency dependence of *ac* conductivity data for **(a)** NBT5, **(b)** NBT10, and **(c)** NBT15 compounds.

Conclusion

Polycrystalline (1-x)$BiFeO_3$–x$Na_{0.5}Bi_{0.5}TiO_3$ x = 0.05, 0.10 and 0.15 were prepared by solid state reaction route method. All these compounds exhibit rhombohedral crystal structure with *R3c* space group. The NTCR character and a non-Debye type relaxation of the compounds was confirmed by the impedance studies. The *ac* conductivity studies unveiled the insulating character of compounds improved with the increase of x. The activation energies estimated from these studies revealed that oxygen vacancies were the main responsible for the conduction in these compounds.

Acknowledgements

TDR is grateful to the UGC, Government of India for the UGC-BRS Research Startup grant [No. F. 30-481/2019(BSR)] and to UGC-DAE CRS, Mumbai Centre, India for research grant under collaborative research scheme [CRS-M-313] to carry out this work.

Conflict of Interest

None.

References

1. Eerenstein W, Mathur ND, Scott JF. 2006. Multiferroic and magnetoelectric materials. *Nature* 442(7104): 759-765. https://doi.org/10.1038/nature05023
2. Catalan G, Scott JF. 2009. Physics and applications of bismuth ferrite. *Adv Mater* 21(24): 2463-2485. https://doi.org/10.1002/adma.200802849
3. Khomskii D. 2009. Classifying multiferroics: mechanisms and effects. *Physics* 2: 20.
4. Neaton JB, Ederer C, Waghmare UV, Spaldin NA, Rabe KM. 2005. First-principles study of spontaneous polarization in multiferroic $BiFeO_3$. *Phys Rev B* 71(1): 014113. https://doi.org/10.1103/PhysRevB.71.014113
5. Thangavelu K, Rao TD, Srinivas A, Asthana S. 2015. Effect of local strain fields on the structural, Néel transition temperature and long range ferroelectric ordering in rare earth substituted $Bi_{0.9}R_{0.1}FeO_3$ multiferroic ceramics (where, R = Gd^{3+}, Tb^{3+}, Dy^{3+}). *J Mater Sci Mater Electron* 26: 8676-8687. https://doi.org/10.1007/s10854-015-3543-9
6. Rao TD, Sattibabu B, Asthana S. 2019. Predicting high magneto-electric coupling in Gd substituted $BiFeO_3$. *Phys Status Solidi B* 256(11): 1900097. https://doi.org/10.1002/pssb.201900097
7. Wang DH, Goh WC, Ning M, Ong CK. 2006. Effect of Ba doping on magnetic, ferroelectric, and magnetoelectric properties in mutiferroic $BiFeO_3$ at room temperature. *Appl Phys Lett* 88(21): 212907. https://doi.org/10.1063/1.2208266
8. Xiang LL, Liu J, Zuo JN, Guo XT, Wang LJ, et al. 2022. Effect of

co-substitution of $Na_{0.5}Bi_{0.5}TiO_3$ and $CaTiO_3$ on the structure and properties of $BiFeO_3$ ceramics. *J Mater Sci Mater Electron* 33(27): 21838-21851. https://doi.org/10.1007/s10854-022-08970-8

9. Dorcet V, Marchet P, Pena O, Trolliard G. 2009. Properties of the solid solution (1-*x*)$Na_{0.5}Bi_{0.5}TiO_3$–(*x*)$BiFeO_3$. *J Magn Magn Mater* 321(11): 1762-1766. https://doi.org/10.1016/j.jmmm.2009.02.014
10. Li LQ, Xiong Y, Tang MH, Cheng CP, Ouyang J. 2014. Effect of $BiFeO_3$ doping on ferroelectric properties of $Na_{0.5}Bi_{0.5}TiO_3$–$BaTiO_3$ based thin film derived by sol-gel method. *J Sol Gel Sci Technol* 72: 394-397. https://doi.org/10.1007/s10971-014-3448-8
11. Rao TD, Asthana S. 2017. Observation of bond enthalpy dependence of insulating character in rare earth substituted $BiFeO_3$. *Mater Res Express* 4(12): 126305. https://doi.org/10.1088/2053-1591/aa9baa
12. Peláiz-Barranco A, Guerra JDS. 2010. Dielectric relaxation related to single-ionized oxygen vacancies in $(Pb_{1-x}La_x)(Zr_{0.90}Ti_{0.10})_{1-x/4}O_3$ ceramics. *Mater Res Bull* 45(9): 1311-1313. https://doi.org/10.1016/j.materresbull.2010.04.026